

Dye versus Quantum Dots in Sensitized Solar Cells: Participation of Quantum Dot Absorber in the Recombination Process

Idan Hod,[†] Victoria González-Pedro,[‡] Zion Tachan,[†] Francisco Fabregat-Santiago,[‡] Iván Mora-Seró,^{*,‡} Juan Bisquert,[‡] and Arie Zaban^{*,†}

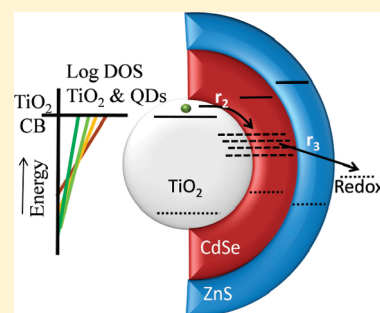
[†]Department of Chemistry, Bar Ilan University, 52900 Ramat Gan, Israel

[‡]Photovoltaic and Optoelectronic Devices Group, Departament de Física, Universitat Jaume I, 12071 Castelló, Spain

S Supporting Information

ABSTRACT: Inorganic quantum dots (QDs) show great potential as absorbers in sensitized solar cell, but there are open questions about the role of quantum dots, where primary electron and hole generation occurs, in the recombination process in this kind of solar cells. In opposition to the conventional dye-sensitized solar cell, here we show that inorganic QDs play a direct role in the recombination process. This fact has been determined by a fingerprint of QDs in the capacitance of the device, where the QDs surface states affect the density of states (DOS) distribution. It indicates that now surface states of QD contribute to the common DOS distribution of TiO₂/QDs/ZnS, which behaves as a single entity, being impossible to distinguish between TiO₂ and QDs. This result highlights the necessity of treating (and optimizing) QD-sensitized solar cells from another perspective than dye-sensitized solar cells, considering the fundamental differences in their behavior.

SECTION: Energy Conversion and Storage



The use of inorganic semiconductors as effective light sensitizers in a dye-sensitized solar cell (DSC)¹ configuration have awakened a great interest in the past few years.^{2–7} Semiconductors present some advantages with respect to conventional dyes, such as high extinction coefficient and large dipole intrinsic moment.⁸ In addition, within the quantum confinement regime, semiconductor nanocrystals or quantum dots (QDs) allow tailoring the light absorption range by the control of QD band gap, achieved by changing their size, shape, or both.⁹ The possibility of obtaining multiple exciton generation (MEG)^{10,11} has also boosted the interest in these materials to overcome the Shockley–Queisser efficiency limit. Despite certain controversy,^{12,13} the recent demonstration of internal quantum efficiencies higher than 100%¹⁴ stresses the potentiality of QDs in QD-sensitized solar cell (QDSC) configuration to produce low-cost and high-performing photovoltaic devices.

The study of the operation mechanisms of QDSCs has relied on the knowledge gained from the field of DSCs, considering QDs in some cases as a simple alternative dye. This approximation/consideration has allowed the demonstration of the concept, but now more accurate understanding is needed to increase the current performance observed in QDSCs. Hodes suggested three main factors that could contribute to differences between DSCs and QDSCs: multiple layers of absorbing semiconductor on the oxide, the different electrolytes normally used for the two types of cell, and charge traps in the absorbing semiconductor.¹⁵ The first factor takes into account the fact that QDs can be prepared and attached to nanostructured TiO₂ in several ways^{5,16,17} and also the possible presence of grain boundaries between quantum dots,¹⁵ whereas the second factor points out the stability of QDSCs.

Many of the semiconductors are not stable with the conventional redox couple (I[−]–I₃[−]) used in DSCs.¹⁵ In addition to the stability issues, interaction of the electrolyte with the QDs, which can change their energy level positions as well as create or passivate surface states, can also affect the ratio between electron injection to the oxide and to the electrolyte, but the change of electrolyte, which can affect significantly the cell performance, does not involve any important change, from the fundamental point of view, between DSCs and QDSCs. The third factor mentioned by Hodes constitutes a significant difference.

In DSCs, photogenerated electrons are quickly injected into nanostructured TiO₂, and the photogenerated holes are regenerated on a time scale that is orders of magnitude shorter than the electron lifetime in TiO₂. In this sense, dyes do not play a direct role in the recombination process of DSCs (Figure 1a). Dyes play an indirect role because their design can favor or hinder injection, recombination, or both.¹⁸ In the case of QDSCs the direct participation of QDs in the recombination process would constitute a fundamental difference with DSCs because this fact necessarily implies a new paradigm in the physical processes involved in the cell operation, pointing out the need for different optimization processes from the ones carried out in DSCs.

Recently we have shown that QDs in QDSC build up chemical potential, which is attributed to charge accumulation in surface traps.^{19,20} The latter seems to interfere with the recombination processes. The groups of Gómez and Toyoda have extensively

Received: October 24, 2011

Accepted: November 16, 2011

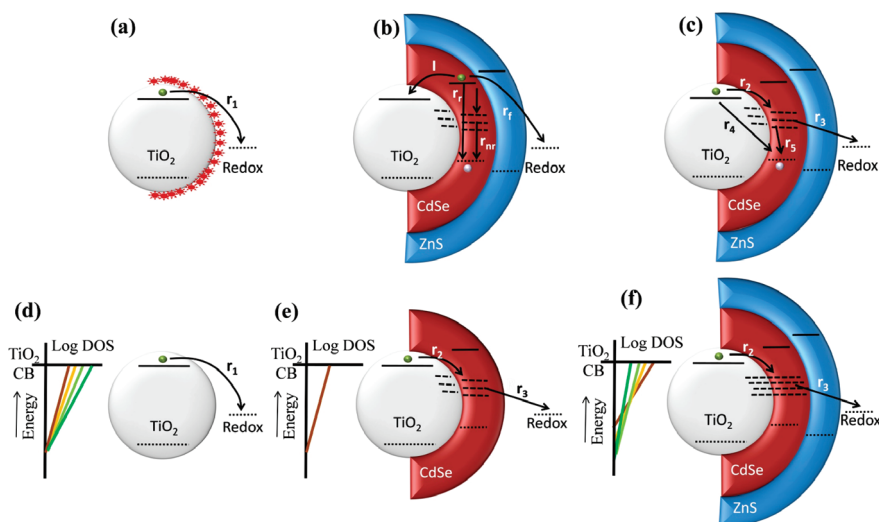


Figure 1. (a) Recombination process in a DSC with good dye regeneration. Electrons in TiO₂ recombine with the acceptor species of the redox couple at a recombination rate of r_1 . (b) Photoexcitation in QDSCs generates an electron (green sphere)–hole (blue sphere) pair in the semiconductor sensitizer. Injection of electron into TiO₂, I , has to compete with several fast recombination pathways such as internal recombination in the QD,²⁴ radiative, r_r , or nonradiative, r_{nr} , with and without previous surface trapping. Another recombination pathway involve the acceptor species in the electrolyte, r_f .^{15,22} Impedance spectroscopy is not sensitive to this recombination path, which can be dramatically reduced by ZnS coating.²² (c) After electron injection to the TiO₂, it can recombine before reaching the extracting contact. With a complete coverage of TiO₂ surface, electrons can react with accepting surface states in the QD, with a recombination rate of r_2 , followed by recombination with holes in the QD, r_5 , or in the electrolyte, r_3 . In addition, electrons in the TiO₂ can recombine directly with holes in the QD, r_4 . (d) Under dark conditions electrons are injected from the contact to the TiO₂. In the case of bare TiO₂ the recombination path way is the same as in conventional DSCs, with a rate of r_1 . (e) After QD deposition, the recombination pathways change. Under dark conditions r_4 and r_5 are not present because of the absence of photogenerated holes in the QD. (f) Finally, ZnS coating reduces the rate of recombination process r_3 . Now TiO₂/QDs/ZnS acts as a single entity. The involvement of the density of states (DOS) in the different situations is also schematically represented for panels d–f using the same colors for each electrolyte as in Figure 2.

studied the photoinjection and recombination in QDSCs with QDs prepared by different methods^{16,21} and with different surface treatments.²² These authors also consider successfully a direct involvement of QD in the recombination process of QDSCs. However, despite an increasing number of indirect proofs pointing out this behavior, there is a lack of direct evidence. In this Letter, we show for the first time that the presence of electrons in the QDs during QDSC operation leaves a signature in the capacitance of the system, measured by impedance spectroscopy (IS), demonstrating a fundamental difference between DSCs and QDSCs. In fact, when the electron recombination from QDs into acceptor species in the electrolyte is sufficiently reduced, it is not possible to distinguish between the chemical capacitance of TiO₂ and QDs, at least in terms of IS characterization. In such a case, both TiO₂ and QDs (experimentally speaking) constitute a single entity involved in the recombination process.

We have systematically studied the recombination process in QDSCs using three different kinds of electrodes: bare TiO₂, TiO₂ covered with CdSe QDs (TiO₂/QDs) and TiO₂ covered with QDs and successively coated with ZnS (TiO₂/QDs/ZnS). CdSe QDs were directly grown on bare TiO₂ electrodes by successive ionic layer adsorption and reaction (SILAR).²³ ZnS was also deposited by SILAR. Seven and two SILAR cycles of CdSe and ZnS were employed, respectively, for electrode preparation. Each kind of electrode was tested in four different polysulfide-based electrolytes (Table 1), which are commonly used in QDSCs.²⁴ All QDSCs were assembled using a Cu₂S counter electrode. Further details of the experimental section and methods are provided in the Supporting Information, SI1. The QDSCs prepared with TiO₂/QDs/ZnS electrodes presented an efficiency of ~3% (SI2 in the Supporting Information),

Table 1. Polysulfide Electrolytes Used in This Study^a

elec	[Na ₂ S] (M)	[S] (M)	[NaOH] (M)	pH	redox potential V vs	
					Ag/AgCl	
E1	1	0.1	1	12.91	–0.687	
E2	1	0.1	0.1	12.88	–0.663	
E3	1	0.1	0	12.99	–0.669	
E4	1	1	0.1	12.96	–0.666	

^aFor redox potential position versus Ag/AgCl, see SI3 in Supporting Information.

indicating that the analyzed cells present a photovoltaic behavior on the order of the state-of-the-art.

Figure 1 displays the different recombination processes expected for QDSCs. After electron–hole photogeneration, fast electron injection and recombination, in addition to trapping, could take place (Figure 1b). As it has been recently pointed out by Guijarro et al.,²² ZnS coating passivates QDs surface traps while reducing the fast internal nonradiative recombination rate, r_{nr} , through trap states and the fast recombination rate with the electrolyte, r_f . After electron injection into TiO₂, it can recombine through several recombination pathways (Figure 1c). Note that we always consider that QDs deposition covers completely the TiO₂ surface. To simplify the system and reduce the number of recombination pathways, we have performed IS characterizations under dark conditions, as in this case there are no holes in QDs. The expected recombination pathways for bare TiO₂, TiO₂/QDs, and TiO₂/QDs/ZnS, under dark conditions, are represented in Figure 1d–f, respectively.

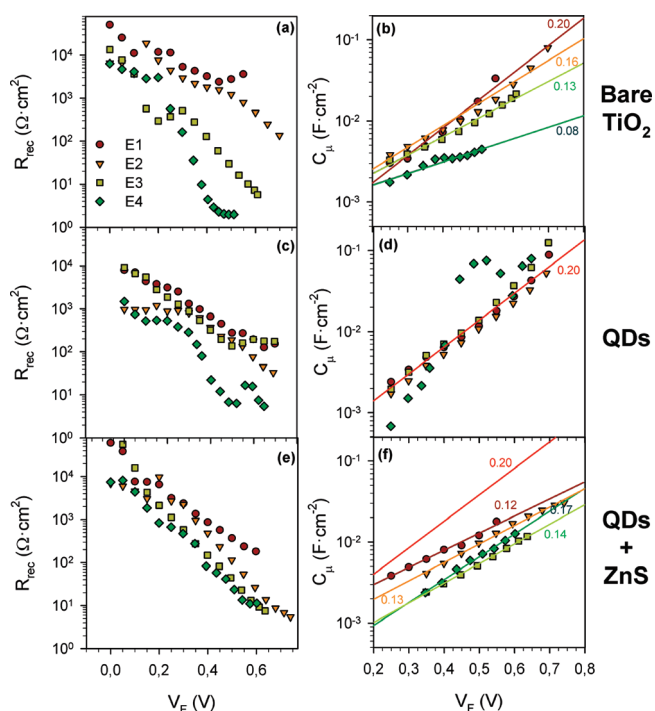


Figure 2. Recombination resistance, R_{rec} , and chemical capacitance, C_{μ} , obtained from impedance measurements²⁵ for QDSCs prepared with bare TiO_2 , TiO_2/QDs , and $\text{TiO}_2/\text{QDs}/\text{ZnS}$ electrodes and different electrolytes (Table 1). R_{rec} includes the combination of the different processes highlighted in Figure 1. Solid lines in capacitance plots are the linear regression fit of the data points with the same colors. The numbers indicated with same color spectrum are the α values.²⁶ For bare TiO_2 electrodes a decrease in the capacitance slope with the number of the electrolyte is observed. For TiO_2/QDs electrodes, independently of the electrolyte used, the capacitance slope is the same and equals the slope obtained for bare TiO_2 and E1. For $\text{TiO}_2/\text{QDs}/\text{ZnS}$ electrodes, regardless of electrolyte type, the capacitance slopes vary from the slope obtained for bare TiO_2 and E1 (this slope is also displayed in the plot, for comparative reasons), indicating a broadening of the $\text{TiO}_2/\text{QDs}/\text{ZnS}$ DOS due to the QDs contribution to the device capacitance.

IS measurements were carried out for the different QDSCs at different applied forward bias. Recombination resistance, R_{rec} , and chemical capacitance, C_{μ} , for each cell as a function of voltage drop in the photoanode (removing the effect of voltage drop in the series resistance), V_{F} ,^{25,26} are plotted in Figure 2. All data were obtained by fitting the IS spectra using the previously described models.²⁵ It is interesting to highlight that the recombination from bare TiO_2 into redox acceptor species varies dramatically with the amount of NaOH and with the amount of S (Figure 2a). For bare TiO_2 samples the slope of C_{μ} (Figure 2b), also varies with the type of electrolyte. This fact implies a change in the DOS of TiO_2 ,²⁶ as indicated in the energy diagram of Figure 1d. Figure 2 also indicates the α values obtained for each sample taking into account that $C = C_0 \exp(\alpha e V_{\text{F}}/kT)$,²⁶ where C_0 is a pre-exponential factor, e is the fundamental charge, k is the Boltzmann constant, T is the temperature, and α is a parameter defining the distribution of surface states. For bare TiO_2 , S electrolyte species broaden the DOS distribution, whereas higher concentration of NaOH prevents the broadening. Note that the differences between the electrolytes cannot be attributed to the change in the redox potential position or to an effect of pH (Table 1). The observed

pH results from the chemical equilibria taking place in polysulfide electrolyte²⁴ (SIS of the Supporting Information). Further research is necessary to understand this behavior, which is not in the scope of this work.

After QDs deposition, the difference in recombination rate (inversely proportional to R_{rec}) between different electrolytes is significantly reduced, being practically the same for E1 up to E3 and increasing slightly for E4 (Figure 2c). C_{μ} for TiO_2/QDs electrodes does not change with the kind of electrolyte, presenting the same DOS and α as obtained for the bare TiO_2 sample with E1 (Figure 2d), except for the case of E4 electrolyte. (See SI4 of the Supporting Information for further discussion on this exception.) From these facts, two conclusions can be extracted: (i) after QD deposition TiO_2 DOS does not change with the type of electrolyte, implying that SILAR totally covers TiO_2 surface, and (ii) after QD deposition very similar recombination resistances are found for all electrolytes. Consequently, the recombination is governed by a charge transfer from TiO_2 to QDs surface states (r_2), independent of electrolyte type (Figure 1e). In other words, recombination of electrons from QDs surface states to the electrolyte (r_3) is faster than the recombination from TiO_2 to QDs surface states ($r_3 > r_2$), knowing that r_3 is electrolyte-dependent. As soon as electrons in the TiO_2 are backinjected into the QDs, they quickly recombine to the electrolyte. As a result, the DOS observed can only be attributed to TiO_2 . It is also important to note that the recombination from bare TiO_2 is not always higher than the recombination from TiO_2/QDs .^{17,22} In fact the ratio r_1/r_2 depends strongly on the type of electrolyte, increasing from E1 to E4. (See SI6 of the Supporting Information.) In addition, this ratio also depends on the preparation of QDs and on the covering of TiO_2 surface with QDs (total or partial).^{16,21}

After ZnS coating, the recombination from QDs surface states to the electrolyte (r_3) is suppressed, producing a reduction in the overall observed recombination (Figure 2e and SI6 of the Supporting Information). As a result, electrons can now accumulate inside the QDs and build up chemical potential. In this situation, it should be expected to observe a fingerprint of QDs in the system capacitance, and this is effectively the observed case (Figure 2f). After ZnS coating, a broadening of DOS, with respect to the TiO_2/QDs electrodes, is observed. Once the TiO_2 surface has been totally covered with QDs, its DOS distribution is not affected by the electrolyte composition. For that reason, the change in DOS observed between TiO_2/QDs and $\text{TiO}_2/\text{QDs}/\text{ZnS}$ samples has to come from the addition of QD DOS. It indicates that now surface states of QD contribute to the common DOS distribution of $\text{TiO}_2/\text{QDs}/\text{ZnS}$, which behaves as a single entity, being impossible to distinguish between TiO_2 and QDs, at least from the impedance characterization point of view. In other words, because of the fact that $\text{TiO}_2/\text{QDs}/\text{ZnS}$ is observed as a single entity, it is now impossible to distinguish between charge accumulated in TiO_2 and charge accumulated in QDs surface states. It is important to highlight that the contribution of QDs occurs when the recombination via the QDs surface is reduced, and consequently the cell performance is enhanced. Under these conditions the operation mechanism of QDSCs is fundamentally different from that of DSCs.

In summary, the recombination from bare TiO_2 to polysulfide redox strongly depends on the type of electrolyte. The electrolyte also affects the TiO_2 DOS distribution. After QD deposition, the surface of TiO_2 is completely covered and the DOS distribution is not affected by the electrolyte. In this case, the recombination is

governed by the electron recombination rate from TiO₂ into QDs, r_2 (independent of the electrolyte), whereas the recombination rate from QDs into electrolyte, r_3 (dependent on the electrolyte), is significantly larger than r_2 . Finally, after ZnS coating, r_3 decreases and electrons stay longer times in the QDs, enabling the observation of DOS distribution in the mixed system; that is, QD's surface states contribute to the common DOS distribution of TiO₂/QDs/ZnS that behaves as a single entity. This demonstration highlights a fundamental difference between DSCs and QDSCs, indicating that the operation mechanisms (and optimizations) of these cells need to be studied from a different perspective.

■ ASSOCIATED CONTENT

S Supporting Information. Experimental section and methods, J - V curves of analyzed cells, redox position against reference electrode Ag/AgCl for aqueous polysulfide electrolytes with $[\text{Na}_2\text{S}] = 1 \text{ M}$, recombination through surface states, some of the chemical and photochemical reactions occurring in polysulfide electrolytes, and recombination resistance for different electrodes in different electrolytes. This material is available free of charge via the Internet at <http://pubs.acs.org>.

■ AUTHOR INFORMATION

Corresponding Author

*E-mail: sero@fca.uji.es (I.M.-S.), zabana@nano.biu.ac.il (A.Z.).

■ ACKNOWLEDGMENT

This work was partially supported by the Ministerio de Educación y Ciencia of Spain under the project HOPE CSD2007-00007 (Consolider-Ingenio 2010) JES-NANOSOLAR PLE2009-0042, and MAT 2010-19827 and by Generalitat Valenciana project PROMETEO/2009/058. I.H., Z.T., and A.Z. acknowledge the support of the Israeli Ministry of Science, Tashtiyot Program.

■ REFERENCES

- (1) O' Regan, B.; Grätzel, M. a Low-Cost High-Efficiency Solar Cell Based on Dye-Sensitized Colloidal TiO₂ Films. *Nature* **1991**, *353*, 737–740.
- (2) Hod, I.; Tachan, Z.; Shalom, M.; Zaban, A. Internal Photo-reference Electrode: A Powerful Characterization Method for Photoelectrochemical Quantum Dot Sensitized Solar Cells. *J. Phys. Chem. Lett.* **2011**, *2*, 1032–1037.
- (3) Tachan, Z.; Shalom, M.; Hod, I.; Ruhle, S.; Tirosh, S.; Zaban, A. PbS as a Highly Catalytic Counter Electrode for Polysulfide-Based Quantum Dot Solar Cells. *J. Phys. Chem. C* **2011**, *115*, 6162–6166.
- (4) Kamat, P. V.; Tvrđy, K.; Baker, D. R.; Radich, J. G. Beyond Photovoltaics: Semiconductor Nanoarchitectures for Liquid-Junction Solar Cells. *Chem. Rev.* **2010**, *110*, 6664–6688.
- (5) Mora-Seró, I.; Bisquert, J. Breakthroughs in the Development of Semiconductor-Sensitized Solar Cells. *J. Phys. Chem. Lett.* **2010**, *1*, 3046–3052.
- (6) Rühle, S.; Shalom, M.; Zaban, A. Quantum-Dot-Sensitized Solar Cells. *Chem. Phys. Chem.* **2010**, *11*, 2290–2304.
- (7) Hetsch, F.; Xu, X.; Wang, H.; Kershaw, S. V.; Rogach, A. L. Semiconductor Nanocrystal Quantum Dots as Solar Cell Components and Photosensitizers: Material, Charge Transfer, and Separation Aspects of Some Device Topologies. *J. Phys. Chem. Lett.* **2011**, *2*, 1879–1887.
- (8) Vogel, R.; Hoyer, P.; Weller, H. Quantum-Sized PdS, CdS, Ag₂S, Sb₂S₃ and Bi₂S₃ Particles as Sensitizers for Various Nanoporous Wide-Bandgap Semiconductors. *J. Phys. Chem.* **1994**, *98*, 3183–3188.
- (9) Robel, I.; Kuno, M.; Kamat, P. V. Size-Dependent Electron Injection from Excited CdSe Quantum Dots into TiO₂ Nanoparticles. *J. Am. Chem. Soc.* **2007**, *129*, 4136–4137.
- (10) Ellingson, R. J.; Beard, M. C.; Johnson, J. C.; Yu, P.; Micic, O. I.; Nozik, A. J.; Shabaev, A.; Efros, A. L. Highly Efficient Multiple Exciton Generation in Colloidal PbSe and PbS Quantum Dots. *Nano Lett.* **2005**, *5*, 865–871.
- (11) Schaller, R. D.; Klimov, V. I. High Efficiency Carrier Multiplication in PbSe Nanocrystals: Implications for Solar Energy Conversion. *Phys. Rev. Lett.* **2004**, *92*, 186601.
- (12) Nair, G.; Chang, L.-Y.; Geyer, S. M.; Bawendi, M. G. Perspective on the Prospects of a Carrier Multiplication Nanocrystal Solar Cell. *Nano Lett.* **2011**, *11*, 2145–2151.
- (13) Trinh, M. T.; Houtepen, A. J.; Schins, J. M.; Hanrath, T.; Piris, J.; Knulst, W.; Goossens, A. P. L. M.; Siebbeles, L. D. A. In Spite of Recent Doubts Carrier Multiplication Does Occur in PbSe Nanocrystals. *Nano Lett.* **2008**, *8*, 1713–1718.
- (14) Sambur, J. B.; Novet, T.; Parkinson, B. A. Multiple Exciton Collection in a Sensitized Photovoltaic System. *Science* **2010**, *330*, 63–66.
- (15) Hodes, G. Comparison of Dye- and Semiconductor-Sensitized Porous Nanocrystalline Liquid Junction Solar Cells. *J. Phys. Chem. C* **2008**, *112* (46), 17778–17787.
- (16) Guijarro, N.; Shen, Q.; Giménez, S.; Mora-Seró, I.; Bisquert, J.; Lana-Villarreal, T.; Toyoda, T.; Gómez, R. Direct Correlation between Ultrafast Injection and Photoanode Performance in Quantum Dot Sensitized Solar Cells. *J. Phys. Chem. C* **2010**, *114*, 22352–22360.
- (17) Mora-Sero, I.; Gimenez, S.; Fabregat-Santiago, F.; Gomez, R.; Shen, Q.; Toyoda, T.; Bisquert, J. Recombination in Quantum Dot Sensitized Solar Cells. *Acc. Chem. Res.* **2009**, *42*, 1848–1857.
- (18) Liu, J.; Zhang, J.; Xu, M.; Zhou, D.; Jing, X.; Wang, P. Mesoscopic Titania Solar Cells With the Tris(1,10-Phenanthroline)-Cobalt Redox Shuttle: Uniped Versus Biped Organic Dyes. *Energ. Environ. Sci.* **2011**, *4*, 3021–3029.
- (19) Shalom, M.; Hod, I.; Tachan, Z.; Buhbut, S.; Tirosh, S.; Zaban, A. Quantum Dot Based Anode and Cathode for High Voltage Tandem Photo-Electrochemical Solar Cell. *Energ. Environ. Sci.* **2011**, *4*, 1874–1878.
- (20) Shalom, M. T., Z.; Bouhadana, Y.; Barad, H.; Zaban, A. Illumination Intensity-Dependent Electronic Properties in Quantum Dot Sensitized Solar Cells. *J. Phys. Chem. Lett.* **2011**, *2*, 1998–2003.
- (21) Guijarro, N.; Lana-Villarreal, T.; Shen, Q.; Toyoda, T.; Gómez, R. Sensitization of Titanium Dioxide Photoanodes with Cadmium Selenide Quantum Dots Prepared by SILAR: Photoelectrochemical and Carrier Dynamics Studies. *J. Phys. Chem. C* **2010**, *114*, 21928–21937.
- (22) Guijarro, N.; Campiña, J. M.; Shen, Q.; Toyoda, T.; Lana-Villarreal, T.; Gómez, R. Uncovering the Role of the ZnS Treatment in the Performance of Quantum Dot Sensitized Solar Cells. *Phys. Chem. Chem. Phys.* **2011**, *13*, 12024–12032.
- (23) Lee, H. J.; Wang, M.; Chen, P.; Gamelin, D. R.; Zakeeruddin, S. M.; Grätzel, M.; Nazeeruddin, M. K. Efficient CdSe Quantum Dot-Sensitized Solar Cells Prepared by an Improved Successive Ionic Layer Adsorption and Reaction Process. *Nano Lett.* **2009**, *9*, 4221–4227.
- (24) Chakrapani, V.; Baker, D.; Kamat, P. V. Understanding the Role of the Sulfide Redox Couple ($\text{S}^{2-}/\text{S}_n^{2-}$) in Quantum Dot-Sensitized Solar Cells. *J. Am. Chem. Soc.* **2011**, *133*, 9607–9615.
- (25) González-Pedro, V.; Xu, X.; Mora-Seró, I.; Bisquert, J. Modeling High-Efficiency Quantum Dot Sensitized Solar Cells. *ACS Nano* **2010**, *4*, 5783–5790.
- (26) Fabregat-Santiago, F.; Garcia-Belmonte, G.; Mora-Seró, I.; Bisquert, J. Characterization of Nanostructured Hybrid and Organic Solar Cells by Impedance Spectroscopy. *Phys. Chem. Chem. Phys.* **2011**, *13*, 9083–9118.